RSC Advances

ROYAL SOCIETY OF CHEMISTRY

www.rsc.org/advances

Cite this: DOI: 10.1039/c0xx00000x

www.rsc.org/xxxxxx

ARTICLE TYPE

A General Method for Mass and Template-Free Production of Hierarchical Metal Oxide Spheres at Room-Temperature

Chao Wang,[a] Mingwei Zhu,*[a] Hong Liu,[b] Yushuang Cui,[a] Yanfeng Chen[a]

Received (in XXX, XXX) Xth XXXXXXXXX 20XX, Accepted Xth XXXXXXXXX 20XX

DOI: 10.1039/b000000x

Hierarchical metal oxide spheres (HMOS) have various applications that stem from their special architectures. Here a novel template-free method is developed for mass fabrication of HMOS at room temperature. It only composes facile processes of PEG modification and self-assembling (PMSA) processes. Its powerful fabrication capability is demonstrated by fabricating HMOS of TiO_2, Fe_2O_3, ZrO_2 and their mixtures with high quality. The related mechanism is investigated and the peculiar PEG configuration on the surface of nanoparitcle is believed to be the origin of the HMOS formation. Several possible applications of HOMS are also exhibited, such as the superhydrophobic property, the enhanced light scattering ability and the improved solar cells performance. Considering the unique fabrication abilities and industrialized mass production potentials, this method may be used as a powerful tool for synthesis of HMOS with extended applications.

1. Introduction

Morphology modification of materials at the nanoscale is an important aspect for materials design and further development of their applications. For the hierarchical architectures, which have dual sizes of the primary nanosizes and the secondary microsizes in the same structure,[1] some size related properties will arise, such as the enhanced light responsibility and increased mass/charge exchange efficiency.[2-4] Benefiting from the unique structures having both high specific surface area and large pore size,[5] they have potential applications in areas of environmental treatments,[6-9] solar cells,[2,5,10,11] energy storage,[3,12] gas/liquid sensing,[4] etc.

Among these hierarchical structures, hierarchical metal oxide spheres (HMOS) are especially useful and therefore a lot of efforts have been focused on their preparations. The most common route for synthesis of hierarchical architectures is template based methods.[13] As a typical fabrication procedure, rigid (colloid spheres, rigid particles, etc.) or soft (liquid droplets, micelles, etc.) materials are used as templates, then they are coated with target materials and finally the hierarchical structures are acquired after removal of the templates. Many hierarchical metal oxide spheres (HMOS) have been synthesized with various materials using this method, such as TiO_2,[14] SiO_2,[15-18] C,[19] ZnO,[20] and Fe_2O_3.[21,22] Template based method is considered as the most promising tool for synthesis of hierarchical architectures because they can efficiently control both the morphology and the microstructure.[3,12] However, the template materials are often high cost and the synthetic procedures are complex and time consuming. Hence, template free methods are rapidly developed for synthesis HMOS of CuO,[23,24] α-FeOOH,[25] TiO_2,[26-31] ZnS,[32] MnS,[33] Fe_2O_3,[34] MnO_2,[35] SnO_2,[36] $Li_4Ti_5O_2$,[37] $SrTiO_3$,[38] NiO,[39] ZnO,[10,11,40] etc. But their synthesis mainly relies on the hydro/solvothermal processes with high temperature or pressure synthesis conditions, which the hydro/solvothermal methods are difficult to be scaled up for mass production. Hence, low temperature synthesis methods are pursued for synthesis HMOS in much milder conditions.[41] Despite these excellent efforts, the synthesis of HMOS is still a challenging field and the acquisition of HMOS is laborious. In view of practical applications, it is highly desirable to develop efficient and cost-effective methods for mass production of HMOS with powerful fabrication capabilities.

In this paper, we introduce a general and facile method for production of HMOS with kilograms fabrication potential. This template-free method mainly contains simple processes of PEG (polyethyleneglycol) modification followed by self-assembling (PMSA). However, HMOS of many materials, or even materials with designed multiple components, can be facilely acquired by this commercial available method. As demonstrations, we have fabricated HMOS with single component of TiO_2, Fe_2O_3, ZrO_2, two-components of TiO_2-Fe_2O_3, and multi-components of TiO_2-Fe_2O_3-ZrO_2 to show the capability and universality of this method for fabrication of different HMOS.

2. Experimental

Preparation of HMOS. As a typical fabrication procedure, metal oxide nanoparticles were mixed with PEG (HO-[CH_2-CH_2-O]$_n$-CH_2-CH_2-OH) in ball milling jars and grinded for 12 hours. Then the powders of 4.0 grams in weight were dispersed in

solution containing 7.0 ml deionized water and 4 drops of nitric acid. After fully dispersion, the paste was coated on the surface of substrate by automatic film applicator coater (ZEHNTNER ZAA 2300) with controllable thicknesses. Then the film was dried and annealed at 450 ℃ for 30 min to remove the organics and other ingredients in the precursors.

Fabrication of dye-sensitized solar cells (DSSC). The electrodes were prepared by coating the TiO_2 pastes on the surface of FTO glass plates by automatic film applicator coater with controllable thickness. After being dried in temperature humidity chamber, the thin film was annealed at 550 ℃ for 30 minutes. The obtained films were absorbed with N719 dye by the vacuum assistant dye adsorption processes. The counter Pt-electrodes was prepared by sputtering Pt catalyst about 3 nm in thickness on the FTO glass. The dye-adsorbed TiO_2 electrode and Pt-counter electrode were assembled into a sandwich type cell and sealed with a hot-melt film (ionomer Surlyn 1702, Dupont) of about 60 μm in thickness. Finally, the electrolye (0.1 M LiI, 0.05 M I_2, 0.5 M 4-tertbutylpyridine in acetonitrile) was filled in and the hole was sealed using the Surlyn 1702 hot-melt film and a cover glass.

Measurements and characterizations. The surface and cross-section morphologies of HMOS were characterized by a scanning electron microscope (SEM, FEI Quanta200 and ZEISS ULTRA 55). The details of the hierarchical TiO_2 spheres were observed by transmission electron microscope (TEM, FEI TECNA1F20 200 kV). The Infrared and diffused reflection spectra were tested by Perkin Elmer spectrophotometer (Spectrum GX) through KBr (Alfa Aesar) wafer method. The static and dynamic contact angles were measured by Contact Angle Meter (OCA30). The Pt counter electrodes were spattered by precision etching coating system (Model 682, Gatan). Photocurrent-voltage characteristics of solar cells were measuredusing a voltage-current source monitor (Orzel Sol 3A, Newport) under illumination by a Newport solar simulator (AM 1.5, 100 mW cm^{-2}) with a scan rate of 10 mV/s.

3. Results and discussion

The PMSA method is schematically illustrated in Fig. 1. Its fabrication procedure mainly contains three steps. Firstly, the metal oxide powder is mixed with PEG (polyethyleneglycol) by ball milling to realize their close contact (step 1). Then the resulted powders are dispersed in water and stirred to provide the condition for nanoparticles self-assembly (step 2). Finally, the resulted HMOS are coated on substrate and the PEG can be removed by sintering (step 3).

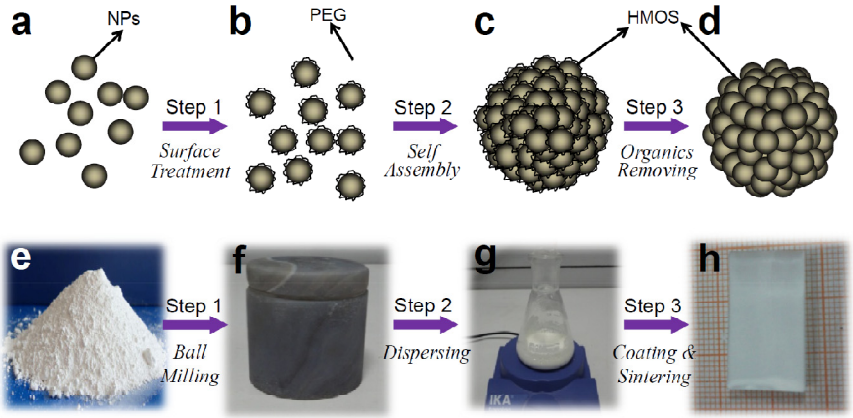

Fig. 1 Schematic illustration and experimental pictures describe the PEG modification and self-assembling (PMSA) method for fabrication of HMOS. The metal oxide nanoparticles (NPs) are firstly modificated with PEG by ball milling (Step 1), then they are dispersed in water to realize self-assembling (Step 2), finally the HMOS are coated on various substrates and remove the organics (Step 3). The corresponding photos show the fabricating processes of hierarchial structures using commercial Degussa P25 nanoparticles as an example.

Fig. 2 shows the SEM and TEM images of the obtained TiO_2, Fe_2O_3 and ZrO_2 hierarchical spheres. Both the surface (Fig. 2a) and cross-section (Fig. 2b) SEM images indicate that the TiO_2 film is completely composed of spherical hierarchical spheres about 1 μm in diameter, morphologically very different form the original TiO_2 nanoparticles (Fig. S1). Each hierarchical sphere is constructed by densely stacked TiO_2 nanoparticles of about 30 nm in diameter (Fig. 2c, 2d). The pore size is about 20 nm (Fig. S2) and the surface area of TiO_2 HMOS is 50.60 m^2/g. Also, the XRD results (Fig. S3) indicate that the PEG removal process by sintering does not change the crystalline structure and inherent properties of metal oxide. Similar structural characters are found in HMOS of ZrO_2 and Fe_2O_3 shown in Fig. 2e and 2f with diameters about 200 nm and 0.8 μm, respectively. All these results demonstrate that the PMSA method is an effective approach for fabricating hierarchical metal oxide spheres.

The most important advantage of our method is that it is facile whereas powerful in mass production of HOMS, which is important for their pratical uses or application area extensions. This advantage stems from the unique characteristics of the method from raw materials to fabrication procedure. The relatively low-price commercial metal oxide nanoparticles are adopted as the starting raw materials. Low-cost and efficient ball

milling mixing process, a way commonly used in laboratories and factories, acts as the main fabrication step. All these characteristics endow the PMSA method with the potentials for industrialized mass production of HMOS. In our demonstrated experiments, the amount of productivity is limited by the capacity

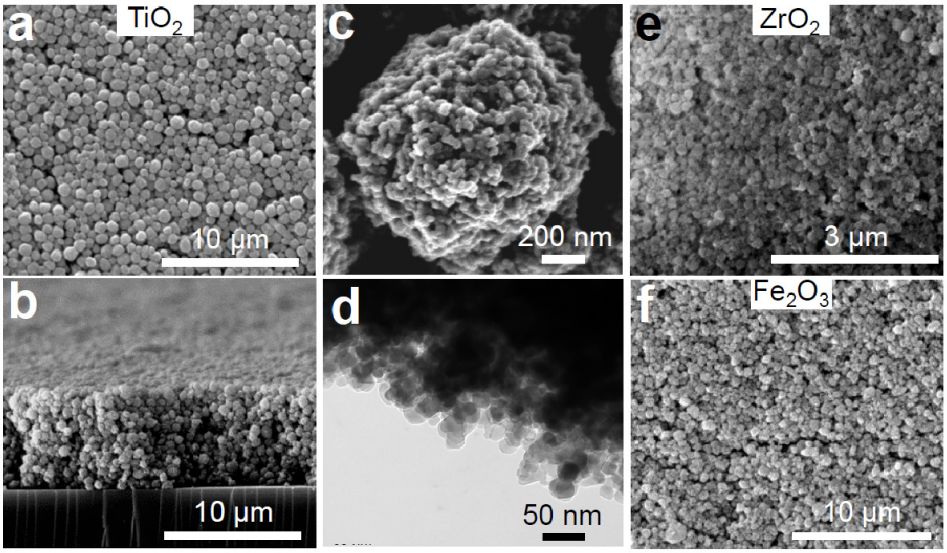

Fig. 2 SEM and TEM images of hierarchical spheres. (a) surface, (b) cross-section and (c) detailed SEM images of TiO_2 hierarchical spheres; (d) TEM image of a typical TiO_2 hierarchical sphere; (e, f) ZrO_2 and Fe_2O_3 hierarchical spheres, respectively. The mass ratio of metal oxide nanoparticles to PEG (molecular weight 20000) is 3:1 during their fabrication.

of the ball mill jars we used. For example, using jar mill of 50 ml, the weights of HMOS of TiO_2, Fe_2O_3 and ZrO_2 are about 21.33 g, 17.37 g and 9.37 g, respectively (Fig. S4). However, We believe that this method can be facilely scaled up and HMOS of kilograms in weight may be efficiently obtained by using much bigger or more ball milling jars.

Another advantage of the PMSA method is that it may create novel HMOS composed of mixtures of different metal oxide nanoparticles. Such mixed poly-nanocrystals may display profoundly improved properties than any of the pure nanocrystal,[14,42-44] but their synthesis is considered to be a challenge. Here we use TiO_2-Fe_2O_3 and TiO_2-Fe_2O_3-ZrO_2 for demonstrations and the results are shown in Fig. S5. These images clearly show that the hierarchical architectures can also form for two-components of TiO_2-Fe_2O_3 and multi-components of TiO_2-Fe_2O_3-ZrO_2. The EDX measurements (Fig. S5) show that the nanoparticles with different materials are mixed together, and each single sphere contains designed kinds of nanoparticles. Such results indicate that different metal oxide nanoparticles jointly participate in the construction of the structures. We believe that the hierarchical spheres can also be fabricated using with various prescriptions for satisfying different application requirements.

The formation of HMOS is surely the result of the minimization of Gibbs free energy in the systerm.[14,32,36] However, we would like to investigate the details in our system. PEG (HO-$[CH_2$-CH_2-$O]_n$-CH_2-CH_2-OH) is often used as surfactant for avoiding aggregation of nanoparticles base on the stereo-hindrance effect. On the contrary, they are the origin for the appropinquity between adjacent nanoparticles. Also, the experments show that the PEG and dry grinding treatment are essential for the HMOS formation and hierarchical structures are not observed if only one of them was used (Fig. S6, S7). Hence we believe that such difference origins from the different configurations that the PEG molecules adsorped on the particle surface. For the commonly used solution adsorption at high surface coverage levels, the "brush" configuration,[45] with one terminal of PEG molecule fixed on the particle surface and the other part extends to the outer solution, is the main manner (Fig 3d). However, for PEG molecule treated by dry grinding process, the "lying" configuration (Fig. 3a), with PEG molecule lies on the particle surface via a number of linkage sites through hydrogen bonding,[46,47] is believed to be the main mode (Fig. S8, infrared transmittance spectra). Such configuration can realize stronger interaction between PEG molecule chain and the nanoparticle. More importantly, the "lying" configuration makes the –OH terminals in PEG molecule fixed on the particle surface and exposes the $[-CH_2$-CH_2-$O]_x$ forming unit outside. This is the key point and it makes the PEG linked nanoparticles display the properties of $[-CH_2$-CH_2-$O]_x$ segment during their interaction or interaction with solvent. Consequently, the aggregation of PEG-linked nanoparticles should be very similar to that of PEO (poly(ethylene oxide) in aqueous solution with segment–segment and segment–solvent interactions. Although the origin of their aggregation is still debated, the hydrophobic interactions [48,49] (the $-CH_2$-CH_2- groups repel water) are believed to serve as the main driving force of the aggregation for PEG-linked nanoparticles in our experiments.

Accordingly, a possible mechanism is proposed to explain the formation of HMOS shown in Fig. 3. Firstly, PEG molecule is bonded on the surface of metal oxide nanoparitcle via a number of linkage sites (Fig. 3a). Then, many tiny "clusters" form after the PEG linked nanoparticles dispered in water (Fig. 3b). Subsequently, these clusters serve as "nuclei" and slowly grow up by continous accepting individual nanoparticles from their surrounding. Finally, hierarchical spheres with certain sizes come into being after all the residual individual nanoparticles used up (Fig. 3c).

Based on the above aggregation formation mechanism, the molecule weight (MW) of PEG, which determines the molecule chain length, may affect the formaion of hierarchical architectures

by changing their surface hydrophobic properties. The shorter the molecule chain, the more negative contribution of the –OH end groups to the hydrophobic interactions of the -CH_2-CH_2- groups. Hence, short chain of PEG should be disadvantageous for the HMOS formation. The experimental results are shown in Fig. S9 using TiO_2 as examples with various molecular weights. Evidently, the hierarchical characteristics weaken gradually with MW decreasing from 20000, 10000, 4000 and finally diminish completely for 2000. Also, surface coverage level can affect

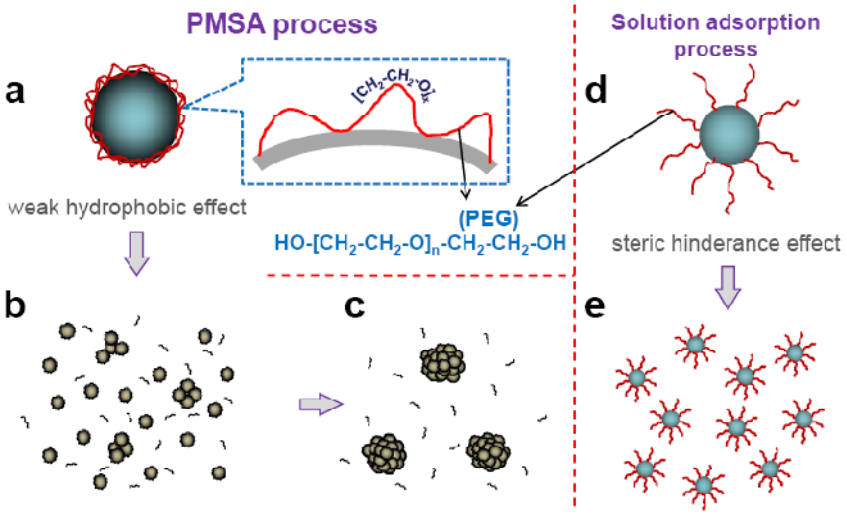

Fig. 3 A possible mechanism for the formation of HMOS. (a) PEG molecule is bonded on the surface of nanoparitcle via a "lying" configuration as a result of dry grinding process. (b, c) The PEG linked nanopartilces produce tiny "clusters" by self-assembling and they subsequently grow up to form hierarchical spheres. (d, e) The "brush" configuration of PEG prevents the particles from aggragation.

the hydrophobic interactions and thereby affect the particle aggregation. However, the mass ratios of TiO_2 to PEG show less important influence on the configuration of the spherical hierarchical structures as shown in Fig. S10.

The uniformity of the resulted aggragates may be interpreted by LaMer model,[50] which is often used for explaining the growth machanism of mono-dispersed submicron particles (Fig. S11). At the starting point, the adjacent PEG linked nanopartilces self-assemble and form many "clusters" within a very short time. This process accompanys by a sharp decrease of the "particle number density" in solution. After that, no new "clusters" are generated because of the enlarged particle distance. The already formed "clusters" gradually grow up and produce uniform particle aggragates.

The resulted HMOS can be facile used without further treatments or requisition for critical construction conditions, equipments, or substrates. They can even be coated on a curved surface of an optical fiber compactly and uniformly (Fig. 4).

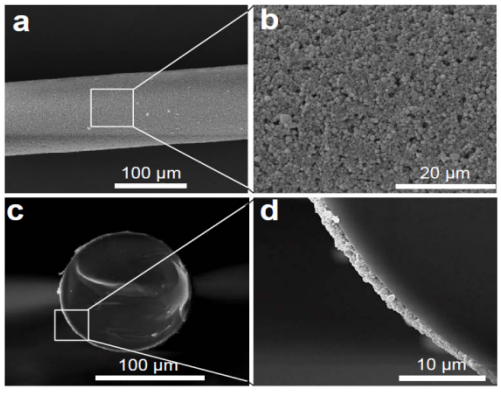

Fig. 4 SEM images of TiO_2 HMOS coated on the surface of a bare optical fiber.

Hence, they can be facile used in many areas. Because TiO_2 is the most intensively studied metal oxide nanomaterials for its wide applications,[51] it is selected to develop the application of HMOS. From the SEM observation in Fig. 2, it is noted that the surface configuration of the HMOS film contains both nano and micron structures, which are very similar to the surface structure of lotus leaf.[52] Therefore, such configurations can be used to bionic the hydrophobic effect of lotus leaf.[53] The as prepared hierarchical TiO_2 spheres are superhydrophilic. However, the HMOS film becomes super-hydrophobic after surface fluoridated (Fig. 5). The measured static contact angle of the TiO_2 film after fluorinating is about 162.6° and dynamic contact angle is about 4°. These values show excellent super-hydrophobic performance, which may be used in self-cleaning and photochemical catalysis.

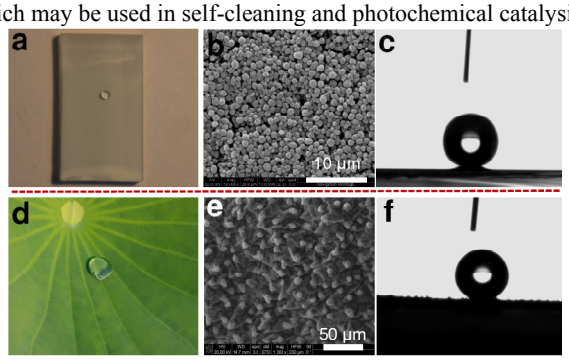

Fig. 5 The contrasts in microstructures and superhydrophobic properties between the film of hierarchical TiO_2 spheres and lotus leaf. The TiO_2 film is surface fluorated before superhydrophobic measurements.

Also, the HMOS have enhanced light scattering capability caused by the microsized architecture in the hierarchical spheres.[54] Fig. 6a and 6b show the schematic and measured diffused reflection spectra for TiO_2 films at different configurations, respectively. The P25 nanoparticle film shows the lowest light scattering efficency, which is rational because their

particle size is far smaller than the wavelenghs of the incident light. For films prepared by using PEG-2000 and 4000, there is little difference in diffused reflection. With the PEG molecular weight increases from 4000 to 20000, the diffused reflection increases by almost 20% at all the visible light wavelengths. Such an increase is in correspondence with the structural evolution from the nanoparticles gradually to hierarchical spheres. Because the band gap of TiO_2 is about 3.2 eV, they cannot absorb the visible light. The increased diffused reflection indicates the stronger light scattering in the film. Hence, hierarchical spheres can improve the light scattering ability proved by the fact that, the more contents of hierarchical spheres in TiO_2 film, the stronger diffused reflection appears. The enhanced light scattering ability can certainly be used to enhance the light harvest of many photo-electron conversion related devices by increasing the probability of interaction between the photons and the light active materials.[10,11] Here we studied the effects of hierarchical structures on the performances of dye-sensitized solar cells (DSSC). From the I-V curves (Fig. 6c) we can see that the short-current densities are enlarged apparently with the increasing of PEG molecule weights. An increase of about 140% for Jsc is observed comparing PEG-20000 sample with the no PEG contrast sample. This trend also corresponds to the light scattering abilities shown in Fig. 6b. In correspondence, shown in table 1, the electrode using TiO_2 hierarchical spheres fabricated by PEG-20000 gives the highest efficiency of 5.30%, which was dramatically higher than the 2.63% obtained for the contrast P25 nanocrystallites. These results indicate that the TiO_2 hierarchical spheres can greatly improve the photovoltaicperformance by enhancing light scattering and harvest. In fact, the enhanced transport of injected electrons and/or the facilitated diffusion of the electrolyte by the hierarchical architecture may also have some contributions.[2] Moreover, it should be noted that the commercial TiO_2 nanoparticles (Degussa P25) were chosen as the basic material for fabrication of DSSC and all the techniques for improving the efficiency were abandoned during the cell fabrication

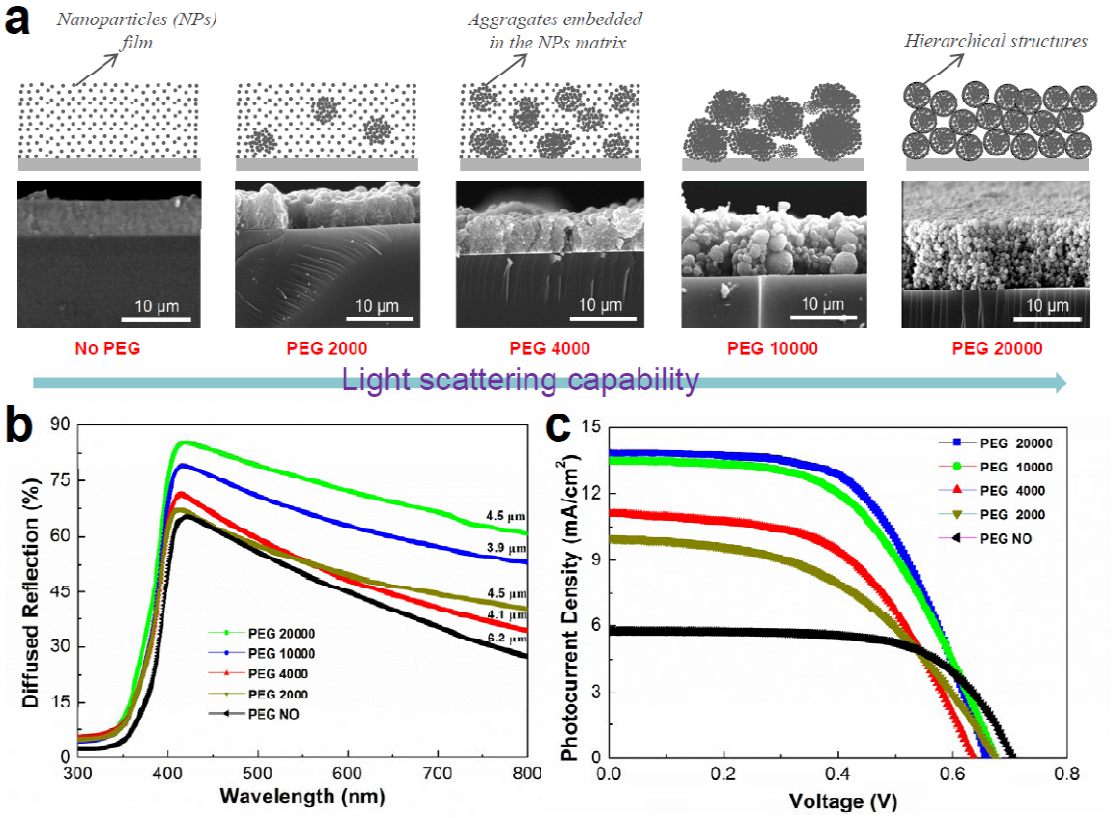

Fig. 6 Schematic film structures (a), mesured diffused reflection spectra (b) and I-V curve (c) of TiO_2 films with different configurations. The films are fabricated by addition of PEG with different molecular weight (green-20000, blue-10000, red-4000, dark yellow-2000, black-no PEG) and the mass ratios of TiO_2 to PEG are fixed to 3:1. The thicknesses of films are also labeled.

Tabel 1 I–V parameters of dye sensitized solar cells with different electrodes.

Sample	Thickness [μm]	Voc[a)] [V]	Jsc[b)] [mA/cm^2]	Fill Factor [%]	Efficiency [%]
PEG-20000	6.2	0.66	13.86	57.93	5.30
PEG-10000	5.7	0.67	13.50	53.97	4.91
PEG-4000	4.9	0.64	11.06	54.07	3.80
PEG-2000	7.1	0.67	9.80	47.65	3.19
PEG-NO	6.5	0.70	5.77	64.60	2.63

a) open-circuit voltage; b) short-circuits current density.

processes. Such designs may further enable the acquisition of reliable results about the effects of TiO_2 hierarchical spheres on the DSSC performances.

4. Conclusion

In summary, we have developed a PMSA method for mass production of hierarchical metal oxide spheres (HMOS). HMOS with single component of TiO_2, Fe_2O_3 or ZrO_2, two-components of TiO_2-Fe_2O_3, and multi-components of TiO_2-Fe_2O_3-ZrO_2 are fabricated to demonstrate the processes and capability of this method. The "lying" configuration of PEG molecule on the particle surface is the key point for the formation of HMOS. Due to the microsized particle diameters, HMOS of TiO_2 show enhanced light scattering ability. When used as electrode in dye sensitized solar cells, a significant improvement of photon-to-current conversion efficiency are achieved compared with P25 nanoparticles. Because of the generality and industrial mass production potential, the PMSA method may enable the synthesis of various interesting HMOS and thereby develop important applications on many fields, such as photocatalysis, solar cells, sensing devices and optics.

Acknowledgements

This work was jointly supported by the State Key Program for Basic Research of China (No. 2013CB632702 and 2012CB921503), National Natural Science Foundation of China (No. 11134006 and 51172105), the Nature Science Foundation of Jiangsu Province (No. BK2011574), and the Priority Academic Program Development of Jiangsu Higher Education Institutions.

Notes and references

[a] *National Laboratory of Solid State Microstructures & Department of Materials Science and Engineering, Nanjing University, Nanjing 210093, China. Fax:+86 2583595535; Tel: +86 2583594317; E-mail: mwzhu@nju.edu.cn*

[b] *State Key Laboratory of Crystal Materials, Shandong University, Jinan 250100, China. E-mail: hongliu@sdu.edu.cn*

† Electronic Supplementary Information (ESI) available: The appearances and weights of the HMOS of TiO_2, Fe_2O_3 and ZrO_2, SEM images of hierarchical spheres of TiO_2-Fe_2O_3, TiO_2-Fe_2O_3-ZrO_2 composites and their corresponding TEM/EDX maps, SEM image of TiO_2 film by wet grinding fabrication process, SEM image of TiO_2 powders after grinding, The infrared transmittance spectra, SEM images of TiO_2 film using PEG of different molecular weights, SEM images of TiO_2 film with different PEG mass ratio, the LaMer model explanation. See DOI: 10.1039/b000000x/

1 T. P. Chou, Q. F. Zhang, G. E. Fryxell and G. Z. Cao, *Adv. Mater.*, 2007, **19**, 2588.
2 Q. F. Zhang and G. Z. Cao, *J. Mater. Chem.*, 2011, **21**, 6769.
3 X. Y. Lai, J. E. Halpert and D. Wang, *E. E. Sci.*, 2012, **5**, 5604.
4 J. H. Lee, *Sensor Actuat. B-Chem.*, 2009, **140**, 319.
5 Y. J. Kim, M. Lee, H. J. Kim, G. Lim, Y. S. Choi, N. G. Park, K. Kim and W. I. Lee, *Adv. Mater.*, 2009, **21**, 3668.
6 J. H. Pan, H. Q. Dou, Z. G. Xiong, C. Xu, J. Z. Ma and X. S. Zhao, *J. Mater. Chem.*, 2010, **20**, 4512.
7 K. Nakata, A. Fujishima, *J. Photochem. Photobiol. B*, 2012, **13**, 169.
8 T. Zhu, J. S. Chen and X. W. Lou, *J. Phys. Chem. C*, 2012, **116**, 6873.
9 Y. Q. Wang, G. Z. Cao, H. Q. Wang, W. P. Cai, C. H. Liang and L. D. Zhang, *Nanotechnology*, 2009, **20**, 155604.
10 Q. F. Zhang, T. P. Chou, B. Russo, S. A. Jenekhe and G. Z. Cao, *Angew. Chem.*, 2008, **120**, 2436.
11 Q. F. Zhang, T. P. Chou, B. Russo, S. A. Jenekhe and G. Z. Cao, *Adv. Funct. Mater.*, 2008, **18**, 1654.
12 Z. Y. Wang, L. Zhou and X. W. Lou, *Adv. Mater.*, 2012, **24**, 1903.
13 W. Wei and Z. Z. Yang, *Adv. Mater.*, 2008, **20**, 2965.
14 X. J. Lv, F. Q. Huang, J. J. Wu, S. J. Ding and F. F. Xu, *ACS Appl. Mater. Interfaces*, 2011, **3**, 566.
15 J. Wang, Q. Xiao, H. Zhou, P. Sun, Z. Yuan, B. Li, D. Ding, A. C. Shi and T. Chen, *Adv. Mater.*, 2006, **18**, 3284.
16 J. G. Wang, F. Li, H. J. X. Zhou, P. C. Sun, D. T. Ding and T. H. Chen, *Chem. Mater.*, 2009, **21**, 612.
17 J. Liu, S. Z. Qiao, S. B. Hartono and G. Q. Lu, *Angew. Chem.*, 2010, **122**, 5101.
18 X. Wu, Y. Tian, Y. Cui, L. Wei, Q. Wang and Y. Chen, *J. Phys. Chem. C*, 2007, **111**, 9704.
19 Q. Li, R. Jiang, Y. Dou, Z. Wu, T. Huang, D. Feng, J. Yang, A. Yu and D. Zhao, *Carbon*, 2011, **49**, 1248.
20 Y. Qiu, W. Chen, S. Yang, B. Zhang, X. X. Zhang, Y. C. Zhong and K. S. Wong, *Cryst. Growth Des.*, 2010, **10**, 177.
21 B. Wang, J. S. Chen, H. B. Wu, Z. Wang and X. W. Lou, *J. Am. Chem. Soc.*, 2011, **133**, 17146.
22 J. Yu, X. Yu, B. Huang, X. Zhang and Y. Dai, *Cryst. Growth Des.*, 2009, **9**, 1474.
23 H. Zhang, Q. Zhu, Y. Zhang, Y. Wang, L. Zhao and B. Yu, *Adv. Funct. Mater.*, 2007, **17**, 2766.
24 R. Liu, J. Yin, W. Du, F. Gao, Y. Fan and Q. Lu, *Eur. J. Inorg. Chem.*, 2013, 1358.
25 B. Wang, H. Wu, L. Yu, R. Xu, T. T. Lim and X. W. Lou, *Adv. Mater.*, 2012, **24**, 1111.
26 W. G. Yang, J. M. Li, Y. L. Wang, F. Zhu, W. M. Shi, F. R. Wan and D. S. Xu, *Chem. Commun.*, 2011, **47**, 1809.
27 Z. Zheng, B. B. Huang, X. Qin, X. Zhang and Y. Dai, *Chem. Eur. J.*, 2010, **16**, 11266.
28 D. H. Chen, F. Z. Huang, Y. B. Cheng and R. A. Caruso, *Adv. Mater.*, 2009, **21**, 2206.
29 J. H. Pan, Z. Cai, Y. Yu and X. S. Zhao, *J. Mater. Chem.*, 2011, **21**, 11430.
30 H. Zhang, H. Yu, Y. Han, P. Liu, S. Zhang, P. Wang, Y. B. Chen and H. Zhao, *Nano Res.*, 2011, **4**, 938.
31 L. S. Zhong, J. S. Hu, L. J. Wan and W. G. Song, *Chem. Commun.*, 2008, **1**, 1184.
32 Q. Zhao, Y. Xie, Z. Zhang and X. Bai, *Cryst. Growth Des.*, 2007, **7**, 153.
33 Y. Cheng, Y. Wang, C. Jia and F. Bao, *J. Phys. Chem. B*, 2006, **110**, 24399.
34 Z. Wu, K. Yu, S. Zhang and Y. Xie, *J. Phys. Chem. C*, 2008, **112**, 11307.
35 P. Yu, X. Zhang, D. Wang, L. Wang and Y. Ma, *Cryst. Growth Des.*, 2009, **9**, 528.
36 Z. J. Miao, Y. Y. Wu, X. R. Zhang, Z.M. Liu, B. X. Han, K. L. Ding and G. Ana, *J. Mater. Chem.*, 2007, **17**, 1791.
37 L. Shen, C. Yuan, H. Luo, X. Zhang, K. Xu and Y. Xia, *J. Mater. Chem.*, 2010, **20**, 6998.
38 Y. Wang, H. Xu, X. Wang, X. Zhang, H. Jia, L. Zhang and J. Qiu, *J. Phys. Chem. B*, 2006, **110**, 13835.
39 X. Song and L. Gao, *J. Phys. Chem. C*, 2008, **112**, 15299.
40 X. Zhao and L. Qi, *Nanotechnology*, 2012, **23**, 235604.
41 Y. Qin, F. Zhang, Y. Chen, Y. Zhou, J. Li, A. Zhu, Y. Luo, Y. Tian and J. Yang, *J. Phys. Chem. C*, 2012, **116**, 11994.
42 M. Agrawal, S. Gupta, A. Pich, N. E. Zafeiropoulos and M. Stamm, *Chem. Mater.*, 2009, **21**, 5343.
43 S. Xuan, W. Jiang, X. Gong, Y. Hu and Z. Chen, *J. Phys. Chem. C*, 2009, **113**, 553.
44 W. W. Wang, Y. J. Zhu and L. X. Yang, *Adv. Funct. Mater.*, 2007, **17**, 59.
45 M. K. Yu, J. Park and S. Jon, *Theranostics*, 2012, **2**, 3.
46 Y. W. Zhang, M. Tang, X. Jin, C. S. Liao and C. H. Yan, *Solid State Sci.*, 2003, **5**, 435.

47 S. Chibowski and M. Paszkiewicz, *Adsorpt. Sci. Technol.*, 2001, **19**, 397.
48 S. Morariu and M. Bercea, *Rev. Roum. Chim.*, 2011, **56**, 545.
49 M. Duval, *Macromolecules*, 2000, **33**, 7862.
50 V. K. LaMer and R. H. Dinegar, *J. Am. Chem. Soc.*, 1950, **72**, 4847.
51 X. B. Chen and S. S. Mao, *Chem. Rev.*, 2007, **107**, 2891.
52 C. Neinhuis and W. Barthlott, *Ann. Bot.*, 1997, **79**, 667.
53 L. Jiang, Y. Zhao and J. Zhai, *Angew. Chem.*, 2004, **116**, 4438.
54 Y. C. Park, Y. J. Chang, B. G. Kum, E. H. Kong, J. Y. Son, Y. S. Kwon, T. Park and H. M. Jang, *J. Mater. Chem.*, 2011, **21**, 9582.